

January 11, 1982

## Nonlinear composition dependence of the Fermi-surface dimensions in alpha-phase copper-germanium alloys

R. Prasad  
*Northeastern University*

A. Bansil  
*Northeastern University*

---

### Recommended Citation

Prasad, R. and Bansil, A., "Nonlinear composition dependence of the Fermi-surface dimensions in alpha-phase copper-germanium alloys" (1982). *Physics Faculty Publications*. Paper 404. <http://hdl.handle.net/2047/d20004181>

## Nonlinear Composition Dependence of the Fermi-Surface Dimensions in Alpha-Phase Copper-Germanium Alloys

R. Prasad and A. Bansil

*Department of Physics, Northeastern University, Boston, Massachusetts 02115*

(Received 3 March 1981)

In considering the  $\alpha$ -Cu<sub>100-x</sub>Ge<sub>x</sub> alloys on the basis of a realistic muffin-tin Hamiltonian, the most notable feature of the electronic spectra is found to be the appearance of an impurity band below the host conduction band. In accord with relevant experiments, a Fermi surface is predicted to grow at approximately half the rigid-band rate for  $x < 0.5$  at.% Ge and essentially at the rigid-band rate for  $x > 5$  at.% Ge. This effect is related to a transition in the nature of states associated with the impurity band; these states are localized atomic  $s$ -like states for  $x \leq 0.5$  and become delocalized in concentrated alloys.

PACS numbers: 71.25.Pi

Alloys of noble metals with polyvalent solutes (such as Zn, Al, Ga, Ge, Si, and As) have played an important role in developing our understanding of the electronic structure of disordered metals.<sup>1</sup> Following the classic studies of Hume-Rothery, similarities in the electronic spectra of this series of alloys have been emphasized and, in fact, the simple rigid-band (RB) model has been used frequently to describe these systems.<sup>1,2</sup> However, recent work shows that the RB picture is deficient in  $\alpha$ -Cu<sub>100-x</sub>Zn<sub>x</sub> in several important respects,<sup>3</sup> most notably, (i) the energy levels in the alloy are complex, with the imaginary part representing disorder scattering, (ii) two sets of  $d$  bands (arising from Cu and Zn  $3d$  levels) appear in the alloy, and (iii) the conduction band of Cu is progressively lowered in energy with respect to the Cu  $3d$  bands as the Zn concentration increases. It is clear then that the host band structure is modified in a concentration *dependent* manner in CuZn. In this connection, we compare and contrast CuGe and CuZn in order to delineate the extent to which the modification of the host spectrum may nonetheless be similar for various polyvalent solutes.

We emphasize that the density of electron states associated with a *single* impurity embedded in Cu differs markedly for the case of various polyvalent solutes.<sup>4</sup> In particular, some impurities yield well-defined impurity levels (e.g., Ge, As, and Si an  $s$  level, and Zn a  $d$  level), while others do not (e.g., Al). This Letter focuses on the question of how the aforementioned differences in the single-impurity limit manifest themselves for *finite* solute concentrations. The symmetry of the impurity levels will be seen to play a dominant role in determining the nature of the alloy spectrum. In this context, one long-standing puzzle is noteworthy. de Haas-van Alphen (dHvA)

experiments of Coleridge and Templeton<sup>5</sup> show that the Fermi surface (FS) of Cu<sub>100-x</sub>Ge<sub>x</sub> grows at roughly half the rigid-band rate in dilute alloys, whereas positron-annihilation experiments<sup>6,7</sup> for higher impurity concentrations find a FS growing in essential accord with the rigid-band model. This is in sharp contrast to the behavior of Cu<sub>100-x</sub>Zn<sub>x</sub> in which the FS grows linearly with  $x$  in agreement with the RB predictions. As noted in the abstract, our computations explain this effect in terms of a transition in the nature of states associated with the Ge impurity band.

We treat Cu<sub>100-x</sub>Ge<sub>x</sub> as a random binary alloy of nonoverlapping muffin-tin atoms. The average electronic spectrum is obtained on the basis of the coherent potential approximation (CPA). The details of such a framework for treating disordered alloys have been discussed elsewhere<sup>8-11</sup> and will therefore not be presented.

Figure 1 shows the CPA complex energy bands along the direction  $\Gamma$  to  $X$  in Cu<sub>90</sub>Ge<sub>10</sub>. The impurity band associated with Ge is seen to appear around  $-0.2$  Ry and is found to involve states of  $s$ - $p$  character.<sup>12</sup> The impurities generally influence host states of  $s$ - $p$  symmetry (e.g.,  $X_4$ ) most severely. In contrast, states of  $d$  character (e.g.,  $X_5$ ,  $X_2$ ,  $X_3$ , and  $X_1$ ) experience smaller shifts and disorder dampings compared to their values in Cu (shown as dashed levels). In view of these results, the nature of disorder in Cu<sub>100-x</sub>Ge<sub>x</sub> can be characterized as follows: states of  $s$ - $p$  symmetry see large disorder (they are in the split-band regime in the sense that two sets of  $s$ - $p$  bands appear in the alloy), whereas the effective disorder parameter for  $d$ -type states is relatively smaller. The situation differs fundamentally from the case of Cu<sub>100-x</sub>Zn<sub>x</sub>,<sup>3,9</sup> where the effective disorder is large for  $d$ -type states (recall that two sets of  $d$  bands appear in Cu<sub>100-x</sub>Zn<sub>x</sub>),

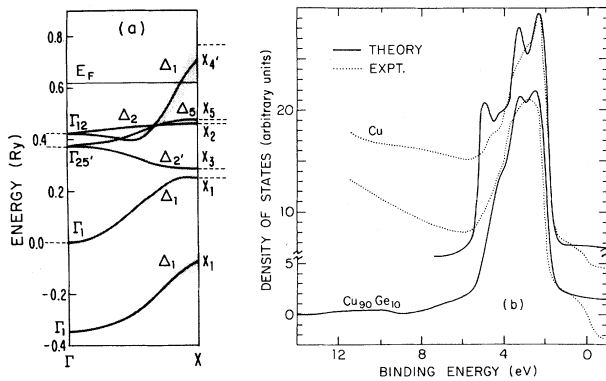


FIG. 1. (a) Complex energy bands along  $\Gamma \rightarrow X$  in  $\text{Cu}_{90}\text{Ge}_{10}$ . The vertical length of shading around the levels equals  $2|\text{Im}E(\vec{k})|$ . Dashed lines on the symmetry points mark energy levels in pure Cu. (b) Average electronic density of states in Cu and  $\text{Cu}_{90}\text{Ge}_{10}$ , together with the corresponding photoemission measurements of Norris and Williams (Ref. 13).

and relatively smaller for the  $s$ - $p$ -type states. This observation is crucial in understanding how solutes with valence  $Z > 2$  modify the spectrum of Cu.

Figure 1(b) shows that the calculated densities of states in Cu as well as  $\text{Cu}_{90}\text{Ge}_{10}$  are in good overall agreement with the photoemission measurements of Norris and Williams<sup>13</sup> (notwithstanding the usual limitations of the neglected matrix-element, many-body, and other effects in the theory). Most notably, the marked broadening of structures at the top and bottom of the Cu  $d$  band in the experimental CuGe spectra (around 2 and 5 eV) is correctly reproduced by the theory. We note that the structure in the density of states arising from the impurity band [around 10 eV in the theoretical curve in Fig. 1(b)] is very weak. This is primarily a consequence of the  $s$ - $p$  character and the previously noted large disorder smearing of the associated states. It is clear that the impurity band would not be observable via usual band spectroscopy techniques. However, the following discussion will show that the concentration dependence of the FS dimensions<sup>14</sup> provides unambiguous evidence of the existence of the impurity band.

Figure 2(a) and Table I show that the predicted slope ( $dk_{\text{neck}}/dx$ ) in the limit of low Ge concentration ( $x < 0.5$  at.%) is in good accord with dHvA measurements.<sup>15-17</sup> (The dHvA results for the belly radii are not available at present.) The CPA neck as well as belly radii are seen to increase at roughly half the corresponding rigid-band rate for quadrivalent impurities [column

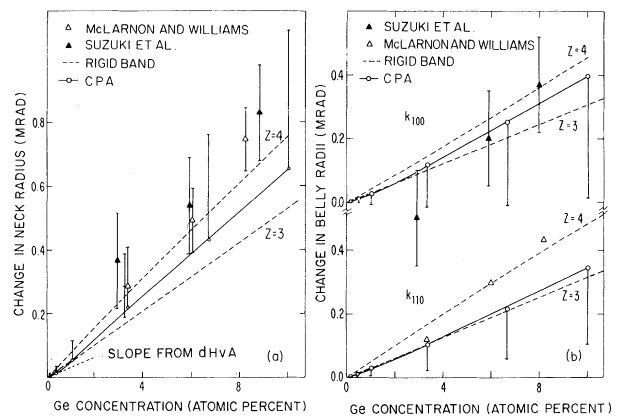


FIG. 2. The CPA results for changes in (a) the neck radius  $k_{\text{neck}}$  and, (b) the belly radii  $k_{100}$  and  $k_{110}$  in Cu as a function of Ge concentration. The disorder smearing  $|\Delta\vec{k}(E_F)|$  is shown by vertical bars attached to the theoretical points (see Ref. 14). Dashed lines give predictions of the RB model for solutes of valence  $Z = 3$  and 4. Experimental points are as indicated in the legend.

(c)] in sharp contrast to CuZn [column (d)]. More precisely, we find the effective valence of Ge in this limit to be 2.5, i.e., only 2.5 of 4 valence electrons of Ge are added at the Fermi energy ( $E_F$ ). This would explain why Coleridge, Holzwarth, and Lee<sup>18</sup> obtain a substantially lower value (than 4) of the Friedel sum in their analysis of CuGe data.

Turning to the high-concentration regime ( $x \geq 5$  at.%), Fig. 2 and Table I show that the calculated slopes ( $dk/dx$ ) of the various FS radii correspond to an effective Ge valence of somewhat less than 4 [seen most easily from column (g) which gives values on the order of unity for the ratio of CPA to the  $Z=4$  RB prediction.] The theoretical values of ( $dk/dx$ ) are in substantial accord with the corresponding experimental values deduced from the positron-annihilation measurements<sup>6,7</sup> [column (f)], despite the relatively poor resolution of the available data.<sup>19,20</sup> It should be noted, nonetheless, that the absolute values of the experimental changes in the FS radii in Fig. 2 are generally higher than the theoretical values [e.g., the calculated neck radius around 9% Ge lies outside the experimental error bars in Fig. 2(a)]. Higher-resolution experiments would be most interesting in this regard.<sup>21</sup>

The nonlinear composition dependence of the FS of  $\text{Cu}_{100-x}\text{Ge}_x$  may be understood as follows. For low Ge concentration ( $x < 0.5$  at.%) the impurity band consists largely of states localized around the impurity. *Qualitatively*, this band may be

TABLE I. The slopes ( $dk/dx$ ) in mrad/at.% Ge for  $k_{\text{neck}}$ ,  $k_{100}$ , and  $k_{110}$ . In the low-concentration regime, theoretical slopes are based on computations with  $x < 0.5$  at.% Ge (the lowest concentration considered was  $x = 0.1$  at.% Ge); the experimental value [column (b)] gives the slope of the straight line drawn through the dHvA data (Fig. 1 of Ref. 5). In the high-concentration regime, theoretical slopes are based on calculations employing  $x > 5$  at.% Ge (see Fig. 2). The experimental values are slopes of straight lines drawn through the positron annihilation data shown in Fig. 2. The quantity of  $r$  is defined as the ratio (CPA slope)/(rigid-band slope).

	Low-concentration regime				High-concentration regime		
	(a) CPA	(b) Expt.	(c) $r(\text{CuGe})$	(d) $r(\text{CuGe})/r(\text{CuZn})$	(e) CPA	(f) Expt.	(g) $r(\text{CuGe})$
$k_{\text{neck}}$	0.04	0.034	0.6	0.6	0.066	0.11, <sup>a</sup> 0.10 <sup>b</sup>	0.9
$k_{100}$	0.02	•••	0.6	0.5	0.044	0.08 <sup>b</sup>	1.0
$k_{110}$	0.02	•••	0.5	0.5	0.039	0.06 <sup>a</sup>	0.8

<sup>a</sup>Based on data of Ref. 6.

<sup>b</sup>Based on data of Ref. 7.

thought of as an atomic  $s$  level, which would accommodate two electrons per Ge atom and yield a FS growing at a rate corresponding to an impurity of valence  $Z - 2$ . (In reality, of course, the impurity band involves some admixture with the host conduction-band states, and therefore, accommodates less than two Ge electrons per impurity and yields a FS growing at a rate somewhat faster than  $Z - 2$ .)

In the regime of higher Ge concentration (i.e.,  $x > 5$  at.%), the states associated with the impurity band become delocalized due to Ge-Ge interaction and develop overlap with the Cu conduction-band states. The modification of the host spectrum can now be grasped better with reference to the molecular orbital theory.<sup>22,23</sup> The  $s$  and  $p$  levels of Cu and Ge interact and form states of bonding and antibonding character. The impurity band incorporates bonding states, while the antibonding states move above  $E_F$ . It follows that the impurity band would now take up roughly one Ge electron per impurity (contrasted with roughly two Ge electrons per impurity in low-concentration limit). But the movement of antibonding states above  $E_F$  causes a loss of roughly one Cu electron per impurity. Thus, on the whole, despite the presence of an additional band (possessing a total weight of two electrons per impurity), the effective valence of Ge is not substantially reduced.<sup>24</sup>

The fact that the impurity band is composed of states of  $s$ - $p$  character would appear to play a crucial role in delocalizing<sup>25</sup> the associated states in concentrated  $\text{Cu}_{100-x}\text{Ge}_x$  and giving a concomitant increase in the growth rate of the FS. Such a transition would not be expected in  $\text{Cu}_{100-x}\text{Zn}_x$

(and does not take place), where the impurity band involves rather tightly bound Zn  $3d$  levels; the width of Zn  $3d$  bands in  $\text{Cu}_{70}\text{Zn}_{30}$  is 1 eV compared to an impurity bandwidth of 4 eV in  $\text{Cu}_{90}\text{Ge}_{10}$ .

We expect our description of the electronic structure of  $\text{Cu}_{100-x}\text{Ge}_x$  to be relevant more generally in describing the effects of Ge, Si, As, and Sn in noble- and transition-metal hosts in the alloy as well as metallic-glass phase. Further investigations of the electronic structure of this class of alloys via various experiments are likely to prove very worthwhile.

We are grateful to L. M. Huisman, S. Kaprzyk, L. Schwartz, and P. E. Mijnarends for important conversations. This work was supported by the U. S. Department of Energy.

<sup>1</sup>For a recent review, see D. J. Sellmeyer, in *Solid State Physics*, edited by H. Ehrenreich, F. Seitz, and D. Turnbull (Academic, New York, 1978), Vol. 33.

<sup>2</sup>See, for example, S. Berko and J. Mader, *Appl. Phys.* **5**, 287 (1975).

<sup>3</sup>A. Bansil, H. Ehrenreich, L. Schwartz, and R. E. Watson, *Phys. Rev. B* **9**, 445 (1974).

<sup>4</sup>R. Zeller and P. H. Dederichs, *Phys. Rev. Lett.* **42**, 1713 (1979); R. P. Lasseeter and P. Soven, *Phys. Rev. B* **8**, 2476 (1973); K. Terakura, *J. Phys. Soc. Jpn.* **40**, 456 (1976).

<sup>5</sup>P. T. Coleridge and I. M. Templeton, *Can. J. Phys.* **49**, 2449 (1971).

<sup>6</sup>J. G. McLarnon and D. Ll. Williams, *J. Phys. Soc. Jpn.* **43**, 1244 (1977).

<sup>7</sup>To. Suzuki, M. Hasegawa, and M. Hirabayashi, *Appl. Phys.* **5**, 269 (1974).

<sup>8</sup>A. Bansil, Phys. Rev. Lett. 41, 1670 (1978), and Phys. Rev. B 20, 4025, 4035 (1979).

<sup>9</sup>R. Prasad, S. C. Papadopoulos, and A. Bansil, Phys. Rev. B 23, 2607 (1981).

<sup>10</sup>R. Prasad and A. Bansil, Phys. Rev. B 21, 496 (1980).

<sup>11</sup>The Cu and Ge potentials were constructed via the usual overlapping charge densities prescription, as in Ref. 9. We avoid further details here because the results and conclusions presented in this article are insensitive to the uncertainties inherent in the first-principles band theory of metals and alloys.

<sup>12</sup>This is not surprising since Ge  $3d$  states are more than 1 Ry below this band.

<sup>13</sup>C. Norris and G. P. Williams, Phys. Status Solidi (b) 85, 325 (1978).

<sup>14</sup>For a discussion of the disorder smearing  $|\Delta\vec{k}(E_F)|$  in an alloy, see Ref. 9.

<sup>15</sup>Special directions method (Ref. 10) was used to carry out the necessary Brillouin-zone integrations. All results reported in Table I employ the 21 direction set. The question of accuracy in low-concentration regime deserves special comment. To this end, several sets of computations on Cu, CuGe, and CuZn using 21 as well as 66 special direction sets (Ref. 10) were carried out for electron per atom values corresponding to 0.1% Ge. Most of these computations were repeated for values appropriate for 0.4% Ge. On this basis we deduce maximum errors of  $\pm 0.01$  mrad/% Ge in  $(d\vec{k}/dx)$  [columns (a) and (b)],  $\pm 0.1$  in  $r$  [column (c); errors are probably much smaller]. We also estimate that the ratio  $r(\text{CuGe})/r(\text{CuZn})$  in column (d) is accurate to  $\pm 0.02$ .

<sup>16</sup>R. G. Poulson, D. L. Randles, and M. Springford, J. Phys. F 4, 981 (1974).

<sup>17</sup>The calculated Dingle temperatures for the (111) neck, and (100) and (110) belly orbits are 257, 211, and 189 K/at.% Ge; the corresponding experimental values (Ref. 16) are  $188 \pm 18$ ,  $109 \pm 8$ , and  $114 \pm 11$  K/at.% Ge. We note that, in contrast to the FS radii, the average disorder scattering does not show a nonlinear composition dependence in the low Ge concentration regime.

<sup>18</sup>P. T. Coleridge, N. A. W. Holzwarth, and M. J. G. Lee, Phys. Rev. B 10, 1213 (1974).

<sup>19</sup>Measurements of decrease in the magnetic moment of Ni diluted by Ge imply an effective Ge valence of approximately 3.5 [J. Crangle and M. J. C. Martin, Philos. Mag. 4, 1006 (1959)], and provide an independent (though indirect) support for the present theoretical predictions.

<sup>20</sup>Crangle and Martin, Ref. 19.

<sup>21</sup>The fact that the host conduction-band states are influenced severely by disorder in  $\text{Cu}_{100-x}\text{Ge}_x$  would make this system an excellent candidate for observing disorder smearing of *positron states* via a positron-annihilation experiment.

<sup>22</sup>See, for example, J. Friedel, Adv. Phys. 3, 446 (1954).

<sup>23</sup>We emphasize that in the dilute limit, the molecular-orbital picture is not a good approximation (see Ref. 22) and it is more appropriate to view the Ge impurity band as a corelike level.

<sup>24</sup>Within the present CPA framework (which is a mean-field theory), the crossover from the low-concentration localized sort of a picture to the high-concentration delocalized picture is a smooth one. Whether the correlations neglected in the theory will yield a sharper transition is a matter for speculation [N. F. Mott, Philos. Mag. 6, 287 (1961)].

<sup>25</sup>Mott, Ref. 24.